Comparison of 3 different bone-borne type expansion appliances used in surgically-assisted rapid palatal expansion: A finite element analysis

Osman Koç,[a] Hande Pamukçu,[b] and Azize Atakan Kocabalkan[b]
Istanbul and Ankara, Turkey

Introduction: This study aimed to compare the effects of 3 different bone-borne type expansion appliances used in the surgically-assisted rapid palatal expansion (SARPE) by finite element analysis. **Methods:** Three different miniscrew-supported palatal expansion appliances were modeled. Median and lateral osteotomies were performed without pterygomaxillary suture separation. Model I consisted of a palatal expander with 2 miniscrews placed 4 mm far from the midpalatal suture. In model II, 2 miniscrews were located at the alveolar ridge between the first molar and the second premolar. In model III, 4 miniscrews were placed as a combination of the first and second models. Stress distributions and amount of displacements were evaluated with Ansys software (version 19.2; Ansys, Canonsburg, Pa) for 5-mm expansion in a symmetrical finite element analysis model to reflect the clinical situation. **Results:** SARPE simulation using miniscrew-assisted maxillary expanders for all models showed a rotation and tipping of the maxilla. The largest displacement was found for the anterior part of the palate in model II and the posterior part in model III. Although a wedge-shaped expansion pattern was observed in all models, this form was more prominent in model II. The highest stress value (0.91 MPa) was measured in model I, and the lowest value (0.004 MPa) was measured in model II for the anterior nasal spine region. The highest stress value (0.51 MPa) was measured in model III, and the lowest value (0.12 MPa) was measured in model II for the posterior nasal spine region. The lowest stress values were measured in model II for all the craniofacial and maxillofacial structures. **Conclusions:** Among the models, the lowest stress distribution conditions for craniofacial and maxillofacial structures were found in model II. The largest displacement was found at the incisors and anterior part of the maxilla for model II. The greatest displacement was found at the posterior region for model III. (Am J Orthod Dentofacial Orthop 2023;163:e23-e33)

Transverse maxillary deficiency is one of the most common orthodontic problems. The treatment protocol may vary according to the severity of the deficiency, age, skeletal maturation, dental condition, and other anomalies accompanying the transversal deficiency.

[a]Faculty of Mechanical Engineering, Yildiz Technical University, Istanbul, Turkey.
[b]Department of Orthodontics, School of Dentistry, Başkent University, Ankara, Turkey.
All authors have completed and submitted the ICMJE Form for Disclosure of Potential Conflicts of Interest, and none were reported.
This study was supported by Başkent University Research Fund (Project No. D-KA21/24).
Address correspondence to: Azize Atakan Kocabalkan, Başkent Üniversitesi Diş Hekimliği Fakültesi, Ortodonti Anabilim Dalı, 11 sok, No. 26, 06490 Bahçelievler, Ankara, Turkey; e-mail, azizeatakan@hotmail.com.
Submitted, March 2022; revised and accepted, December 2022.
0889-5406/$36.00
© 2022 by the American Association of Orthodontists. All rights reserved.
https://doi.org/10.1016/j.ajodo.2022.12.001

Maxilla can be expanded with slow or rapid expansion appliances if the sutura palatina media has not completed its skeletal maturation. When sutural fusion occurs, only surgically-assisted expansion can be achieved. Surgically-assisted rapid palatal expansion (SARPE) is preferred in nongrowing adolescents and adults for orthopedic expansion by reducing the resistance in the sutures.[1] SARPE produces stable widening of the maxilla and is an extremely effective method for skeletal expansion in patients with fully fused midpalatal sutures.[2] This method is also one of the modalities of gaining space for the teeth to be in the correct position.[3,4] This acquisition occurs mainly with lateral rotation of the right and left parts of the maxilla and minimally with horizontal movement.[5]

The forces applied with the expansion appliances can cause undesirable side effects such as dental tipping, fenestration, resorption, and relapse in the supported

areas.[6,7] In recent years, the usage of orthodontic skeletal anchorage appliances such as miniscrews and miniplates has allowed the design of maxillary expansion appliances that can create skeletal expansion while minimizing undesirable effects on teeth.[8] Successful maxillary expansion of miniscrew-supported maxillary expander appliances has been reported in most studies emphasizing increasing maxillary arch width without notable adverse effects on teeth and periodontium.[9-11] Today, bone-borne expansion appliances are the primary choice for eliminating the side effects in nongrowing adolescents and adults.[12,13]

Miniscrew stability is critical for successful bone-borne expansion, as it is important in all orthodontic treatments. Miniscrew loss and/or loosening rates were found between 6.9%-28% in the previous literature, and their success depends on many different factors such as amount and direction of applied force, insertion site, quality of bone, patient's age, operator's experience, length, diameter, and shape of miniscrew.[14-22]

The position of the miniscrew is an important factor in the expansion and design of the expansion appliance. Although many bone-borne expansion appliances have been developed, the areas for miniscrew insertion in the palatal bone are limited. Mostly preferred insertion areas for miniscrews are the alveolar process and the anterior part of the palate. The T-zone in the anterior palate is one of the most suitable areas for symmetrical anchorage requirements.[23-25] This area allows greater stability with high bone quality and thin soft tissue, has a low risk of contact with roots, and is advantageous because of its distance from anatomic structures.[26,27] Alternatively, the interradical region between the first molar and second premolar was suitable for miniscrew applications because of the large interradicular space, wide cortical plate, and thin palatal tissue.[24]

The finite element method (FEA) is an engineering technique used for the calculation of stress and deformation on complex structures and is an important tool that can be used in the field of orthodontics. With the help of FEA, the amount of displacement occurring in the maxilla and the change in the stress occurring in the surrounding structures can be evaluated.

This FEA study aimed to compare the effects of 3 different bone-borne type expansion appliances (with variations in the number of miniscrews and their anatomic locations) used in SAPRE. The null hypothesis of the present study is that no differences exist for the effect of the different bone-borne expansion appliances.

MATERIAL AND METHODS

This study was approved by Başkent University Institutional Review Board (Project no. D-KA21/24) and supported by Başkent University Research Fund.

An anatomic model of a male skull in the stereolithography file format has been downloaded from an open source (BodyParts3D project; University of Tokyo, Tokyo, Japan).[28] Teeth, facial and cranial bones were downloaded, and all bones (frontal, parietal, sphenoid, ethmoid, nasal, lacrimal, zygomatic, occipital) were combined except the maxilla with Ansys software (version 19.2; Ansys, Ansys, Canonsburg, Pa).

The PDL with a thickness of 0.2 mm was modeled with the help of the offset command.[29] The maxilla, teeth, and PDLs were independently included in the overall model, and a symmetrical model of the craniofacial and maxillofacial structures has been created for FEA (Figs 1, *A* and *B*).

According to the literature review of FEA studies, there is no need to calculate sample size and study power in FEA studies.[30-32] Because for every study group, 1 standardized model is constructed at the beginning of the study, and all tests are applied to the same group model in a standard way.

Three miniscrew-supported palatal expansion appliances were designed with FEA to compare SARPE simulation results; median and lateral osteotomies were performed in these models without pterygomaxillary suture separation (PTMS) (Fig 1, *C*).

1. In model I, 2 miniscrews of the expander were placed 4 mm far from the midpalatal suture at the palatal ridge, between the canine and first premolar (Fig 1, *C*).
2. In model II, 2 miniscrews were located at the alveolar ridge between the first molar and the second premolar and 6 mm far from the alveolar crest (Fig 1, *C*).
3. In model III, 4 miniscrews were placed as a combination of the first and second models (Fig 1, *C*).

Miniscrews with the same diameters (diameter, 1.6 mm; length, 12 mm) were used on all models for standardization, and these screws were modeled with Ansys software.

Cortical and cancellous bone were considered anisotropic; tooth, PDL, and stainless steel were homogeneous and isotropic. The material properties of each previously mentioned component can be found in Table I.[21,29,33,34]

The coordinates were defined using the anteroposterior axis as the x-axis, the longitudinal or vertical axis as the y-axis, and the transverse axis as the z-axis. Each

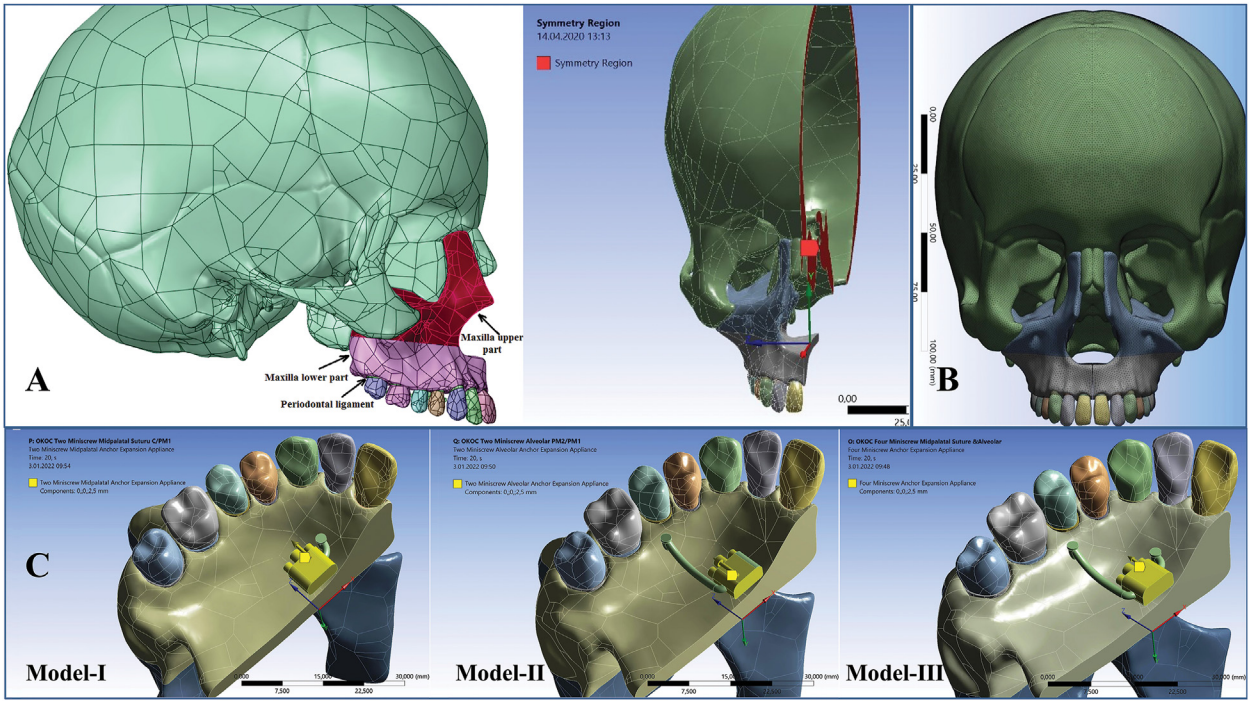


Fig 1. A, Symmetrical model of craniofacial structures; **B,** Frontal views of the model divided into quadratic tetrahedral mesh elements; **C,** Model I: 2 miniscrews were placed 4 mm near the midpalatal suture region, model II: 2 miniscrews were placed close to the alveolar crest, and model III: 4 miniscrews were placed close to the alveolar crest and the midpalatal suture.

Table I. Finite element model's material properties

Anatomic structure	*Material properties (MPa)*		
Cortical maxillary bone	Ex: 12,000	Vxy: 0.18	Gxy: 3600
	Ey: 11,640	Vyz: 0.40	Gyz: 5400
	Ez: 15,600	Vxz: 0.30	Gxz: 4100
Cortical skull bone	Ex: 12,580	Vxy: 0.48	Gxy: 4400
	Ey: 13,600	Vyz: 0.24	Gyz: 6700
	Ez: 21,200	Vxz: 0.32	Gxz: 4900
Cancellous bone	Ex: 1148	Vxy: 0.32	Gxy: 434
	Ey: 1148	Vyz: 0.05	Gyz: 68
	Ez: 210	Vxz: 0.05	Gxz: 68
Dentin	19890	0.31	
PDL	50	0.49	
Stainless steel	193000	0.35	

E, elastic; *x*, x-axis (anteroposterior); *V*, Poisson's ratio; *y*, y-axis (longitudinal or vertical); *G*, Shear modulus; *z*, z-axis (transverse dimensions).

deformed state and different stress levels were shown using different color scale bands.

The values of von Mises stress, which show the possibility of yield and deformation of teeth and bones, were measured in MPa, and displacements were measured in mm. In transient structural analysis (dynamic analysis), geometric nonlinear theory, nonlinear contact theory, and nonlinear materials methods were used to evaluate displacements and von Mises stress distribution. Displacement and stress values were evaluated with Ansys software on the same element using a probe in all models.

The foramen magnum was completely fixed on serving as the origin point.[32] The displacement movement was transmitted to the maxilla with the miniscrews, and the expansion screw was activated by 0.25 mm in all

Table II. Finite element model's element, nodes, mesh size (mm), and average skewness element quality convergence values

Anatomic structure	*Average skewness value*	*Nodes*	*Element*	*Mesh size (mm)*
Skull	0.15	1691902	1158657	1.8
Maxilla (lower part)	0.17	105921	71404	1.3
Maxilla (upper part)	0.15	104642	71184	1.3
PDL	0.4	95057	47053	0.6
Tooth	0.18	159921	106775	0.8
Miniscrew	0.24	10020	5944	0.6

models. A transversal displacement of 2.5 mm was achieved in the z-axis, corresponding to 5 mm of movement in the symmetrical FEA model. Results were obtained after a total activation of 5 mm. A frictionless contact was defined between the maxillary surfaces decoupled by lateral osteotomy in all models.

Bonded contacts were defined between the maxilla and teeth, PDL, and expansion appliance's screw. They move as a single unit, no sliding or separation between faces and edges were allowed.

The amount of rotation for the maxilla was measured from angular changes made by the line passing through the nodes between the anterior nasal spine (ANS) and posterior nasal spine (PNS) points according to the symmetrical plane of the skull.

Quadratic tetrahedral elements were used for volumetric mesh generation, and the FEA model was divided into 2,167,463 nodes and 1,461,017 elements (Fig 1, *B*). Element, nodes, and mesh size values were the same for all models, and the average mesh skewness element quality convergence value was set to 0.16 (Table II). The spectrum of the skewness mesh metrics is shown in Figure 2.

Mesh refinement was performed at the contacting surface of the maxilla and sphenoid bone. The element mesh size was determined as 1.3 mm at the contact surface of the sphenoid bone and 1 mm at the contact surface of the maxilla.

RESULTS

The largest amount of displacement was seen at the level of the central incisors, and transversal displacements of the incisors were larger than the posterior teeth in all models (Table III). Our null hypothesis was rejected because the largest displacement values were measured at the central incisors and ANS in model II for all axes. The maximum displacement value at the PNS levels was measured in model III for the z-axis (Table III; Fig 3; See Videos 1, 2, and 3, available at www.ajodo.org).

SARPE simulation that uses miniscrew-assisted maxillary expanders for all models showed a rotation and tipping of the maxilla (Table III; Fig 3; See Videos 1, 2, and 3, available at www.ajodo.org). Although a wedge-shaped expansion pattern was observed in all models, it was more prominent in model II. The highest angular rotation value was measured for model II (Table III).

Model II showed a pattern that has the minimum stress concentration (38.4 MPa) in the miniscrew region, but model I showed the maximum stress concentration (157.9 MPa) in the same region (Table IV). The stress was concentrated more at the medial pterygoid plate than at the lateral pterygoid plate in all models. Among all models, the highest stress values were measured in model III for the medial pterygoid plate region (Table IV).

The lowest von Mises stress values were measured in the ANS and PNS regions for all models (Table IV). The highest von Mises stress value (0.91 MPa) was measured in model I, and the lowest value (0.004 MPa) was measured in model II for the ANS region. The highest von Mises stress value (0.51 MPa) was measured in model III, and the lowest value (0.12 MPa) was measured in model II for the PNS region. The minimum stress value was measured in model II for all the craniofacial and maxillofacial structures among the models (Table IV; Figs 4-6).

The maximum mean elemental stress values formed in the models were fairly high (490 MPa, 452 MPa, and 435 MPa for models III, II, and I, respectively). Elements with higher stress values (*red* in figures) and elements with structural errors were found to be the same. When the maximum stress locations of the models were examined, it was observed that the stress accumulated at the nodes and in a few elements of that volume.[25,35-37]

Mesh convergence was performed in the maximum stress regions to optimize the accuracy and duration of the solution. According to mesh convergence results, the elemental mean stress value measured in the region with the highest stress did not change >6%. This shows that the optimum number of elements has been determined for the model.

DISCUSSION

The maxillary expansion could be affected by factors such as the type of expansion appliance, the patient's age, gender, bone density, maturity of the midpalatal suture, and tonicity of muscles and soft tissues.[29,30,38] Some of these factors cannot be included in FEA studies. This study includes a mathematical model on the basis of



Fig 2. Skewness mesh metrics spectrum.

Table III. The unilateral displacements (mm) based on the direction after 5 mm of activation of the bone-borne palatal expander in all models

	Model I			*Model II*			*Model III*		
Anatomic structure	*x*	*y*	*z*	*x*	*y*	*z*	*x*	*y*	*z*
Central incisor	0.298	−0.111	3.447	1.339	−0.388	4.927	0.183	−0.046	3.492
Lateral incisor	0.088	−0.023	3.303	0.929	−0.288	4.672	−0.018	0.082	3.375
Canine	−0.167	0.094	3.065	0.473	−0.193	4.255	−0.242	0.191	3.143
First premolar	−0.301	0.165	2.661	0,267	−0.126	3.571	−0.351	0.268	2.815
Second premolar	−0.480	0.223	2.332	−0.014	−0.063	3.030	−0.503	0.338	2.549
First molar	−0.438	0.276	1.980	0.058	0.005	2.466	−0.468	0.403	2.245
Second molar	−0.369	0.298	1.443	0.160	0.036	1.616	−0.402	0.428	1.738
ANS	0.451	−0.206	2.887	1.487	−0.467	4,102	0.280	−0.158	2.828
PNS	0.522	−0.013	0.771	1.628	−0.275	0,671	0.366	−0.117	1.046
Frontomaxillary suture	−0.208	0.280	0.003	0.003	−0.010	0.000	−0.259	0.418	0.002
Zygomaticomaxillary suture	−0.087	0.308	0.049	0.012	0.008	0.021	−0.034	0.481	0.103
Frontozygomatic suture	−0.216	0.272	0.005	−0.001	−0.002	0.002	−0.293	0.411	0.011
Zygomatic arch	−0.124	0.162	0.008	−0.002	−0.005	0.000	−0.149	0.230	0.006
Medial pterygoid plate	−0.422	0.235	0.212	0.044	−0.014	0.044	−0.436	0.354	0.329
Lateral pterygoid plate	−0.280	0.292	0.117	0.010	−0.004	−0.010	−0.358	0.402	0.152
Foramen magnum	0.000	0.000	0.000	0.000	0.000	0.000	0.000	0.000	0.000
Angle of rotation and tipping	−2.96°			−4.81°			−2.55°		

Note: Positive values indicate forward, outward, or upward displacement. Negative values indicate backward, inward, or downward displacement. Median and lateral osteotomies were made in all models without pterygomaxillary suture separation; for model I, 2 miniscrews were placed 4 mm near the midpalatal suture region; for model II, 2 miniscrews were placed close to the alveolar crest; and for model III, 4 miniscrews were placed close to the alveolar crest and the midpalatal suture.
x, x-axis (anteroposterior); *y*, y-axis (longitudinal or vertical); *z*, z-axis (transverse dimensions).

the human skull and represents the clinical situation of an adult patient to rationalize SARPE treatment without PTMS.

Stable and safe palatal miniscrew insertion areas have been determined in the literature.[23-25] The anterior palate appears to be one of the best sites for inserting orthodontic miniscrews or palatal implants. Another alternative is the palatal alveolus between the maxillary first molar and second premolar. In this site, the favorable position of the first molar's palatal root and the buccal angulation of the second premolar provides excellent access for the direct insertion of a miniscrew.[24] In this study, 3 different expansion appliances supported by miniscrews were compared and inserted into these safe areas; expansion appliance designs were applied to the FEA model, and the clinical situation was simulated with the correct modeling of anatomic structure, boundary conditions, and material properties. With lateral osteotomy, there is a bone loss between the maxillary bones as much as the saw thickness. In this study, frictionless contact between the 2 bone surfaces was defined, and none of the similar FEA studies defined frictionless contact. Even if the frictional contact between these 2 surfaces were defined, there would be no significant difference in the results.[39]

The FEA is an accurate simulation for evaluating surgical procedures performed on the facial skeleton.[40] However, in FEA studies, it is very important to specify the boundary conditions (type of contacts, applied forces, amount of displacement), material properties, mesh structure (no. of elements and nodes), and mesh convergence for the reliability of the results and the reproducibility of the analysis. Especially, the mesh of FEA has a direct effect on the accuracy of the solution. According to the mesh metrics spectrum created by Ansys software, mesh convergence was required to produce reliable results.[35,41] Mesh convergence refers to the number of elements that must be present in the model,

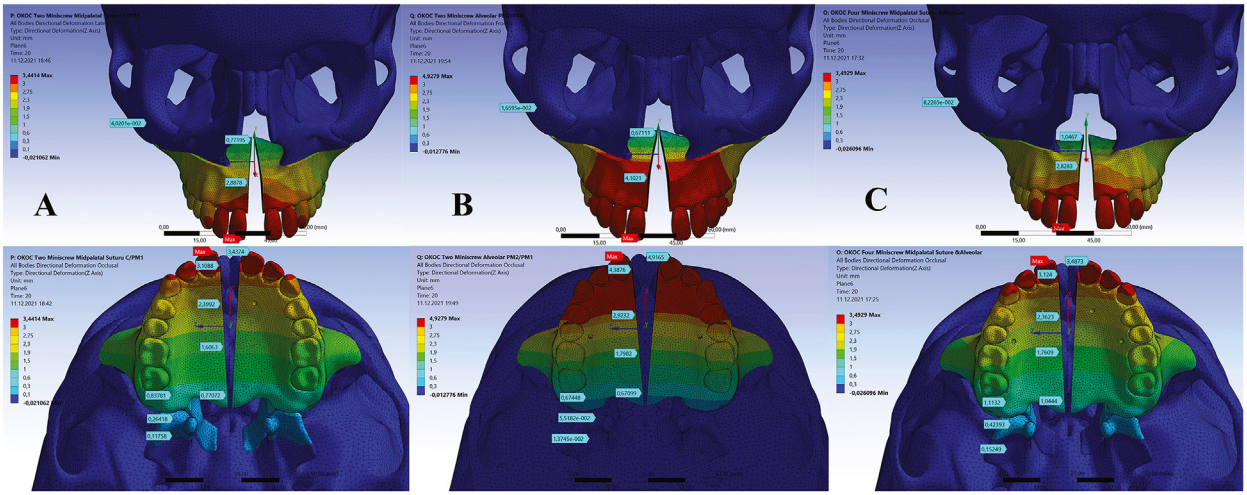


Fig 3. A, Model I: Unilateral displacement (frontal, occlusal); **B,** Model II: Unilateral displacement (frontal, occlusal); and **C,** Model III: Unilateral displacement (frontal, occlusal).

Table IV. The mean elemental stress (von Mises stress and first principal stress) distribution (MPa) in craniofacial and maxillofacial structures after 5 mm of activation of the bone-borne palatal expander in all models

	Model I		*Model II*		*Model III*	
Anatomic structure	*Von Mises stress*	*First principal stress*	*Von Mises stress*	*First principal stress*	*Von Mises stress*	*First principal stress*
Frontomaxillary suture	6.826	7.356	1.171	1.074	7.811	8.664
Zygomaticomaxillary suture	1.080	1.021	1.034	0.182	6.264	2.399
Frontozygomatic suture	11.10	−0.484	2.509	−0.111	19.97	−0.967
Zygomatic arch	13.78	0.107	0.410	0.141	6.793	0.168
Nasal frontal suture	11.25	11.60	1.454	1.681	14.492	16.79
Medial pterygoid plate	134.8	40.91	46.512	13.409	154.04	36.94
Lateral pterygoid plate	124.8	7.068	22.468	4.445	140.76	14.70
Maxillary tuberosity	5.335	3.101	1.614	0.914	16.082	11.55
PNS	0.375	0.435	0.126	0.138	0.516	0.009
ANS	0.915	0.034	0.004	0.000	0.085	0.500
Miniscrew region	157.9	93.54	38.482	10.888	77.837	47.75

Notes: Positive values indicate compression stress value, whereas negative values indicate tensile stress value.

and mesh size changes do not affect the analysis results.[35,37] Spectrum of the skewness mesh metrics of the study is shown in Figure 2, and low orthogonal quality and high skewness values are not recommended. The accuracy of the analysis results is influenced by these values, and the accuracy decreases as the average skewness value progresses from excellent to good. The average skewness element quality and mesh convergence values of all parts forming the geometry of the model were excellent for this study.

Transient structural (dynamic) analysis can be used to measure the dynamic response of a structure under the influence of time-dependent load. Dynamic analysis can determine time-varying displacements, strains, stresses, and forces in a structure responding to a transient load.[35,42] In this study, the effect of the expansion on the craniofacial structures was examined, which depends on time (20 seconds in total), and 1 turn of the expansion screw corresponds to 1 second.

A large number of expansion appliance designs have been described in the literature. However, it is impossible to define the ideal expansion appliance. A previous FEA study evaluated the effect of 4 different maxillary expansion appliances and exhibited significant differences among the miniscrews.[29] All appliances demonstrated downward displacement and horizontal movement in

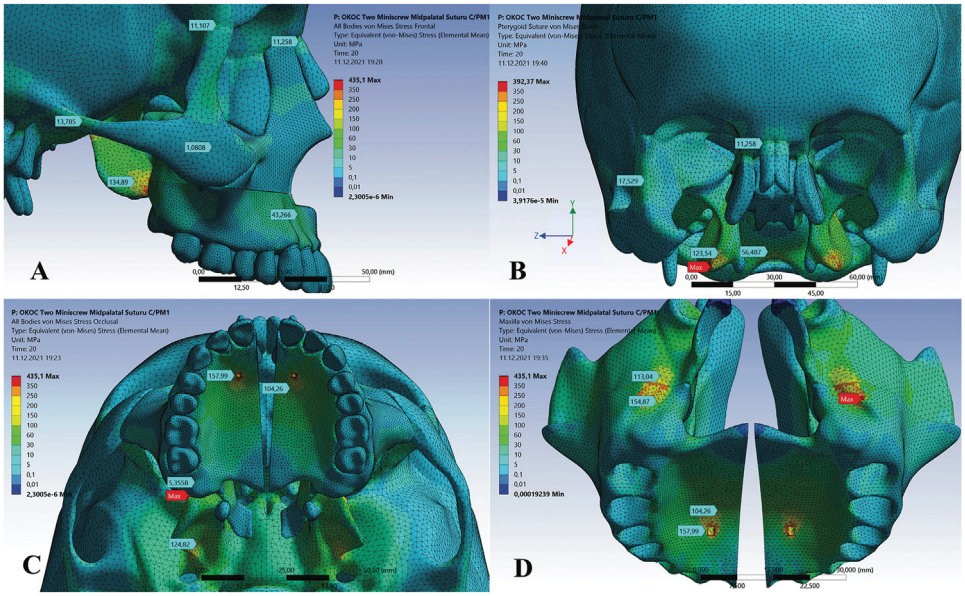


Fig 4. **A** and **C,** Model I: Unilateral stress distribution in the craniofacial structures and maxillofacial sutures; **B** and **D,** Unilateral stress distribution in the pterygomaxillary suture and screw region after 5-mm activation of the bone-born expansion appliance.

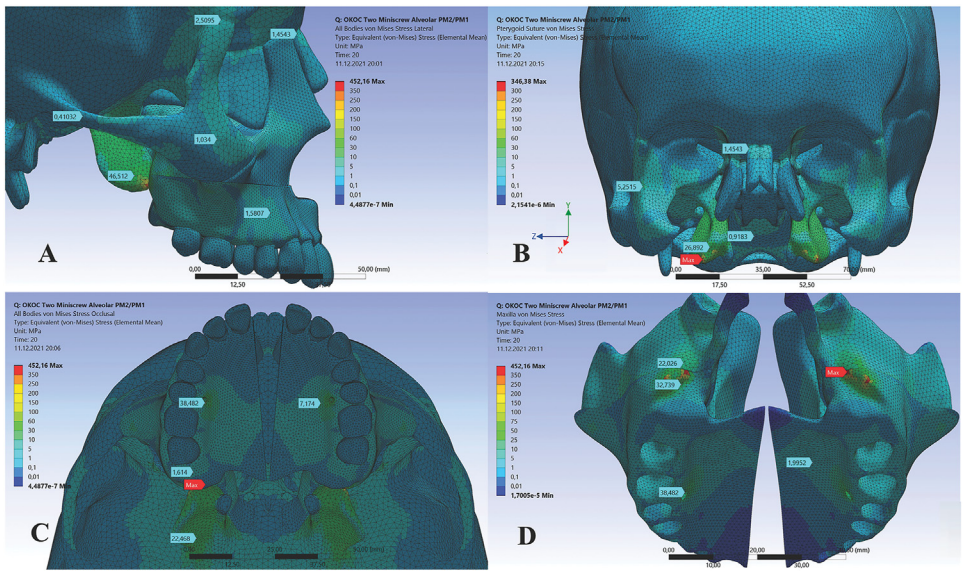


Fig 5. **A** and **C,** Model II: Unilateral stress distribution in the craniofacial structures and maxillofacial sutures; **B** and **D,** Unilateral stress distribution in the pterygomaxillary suture and screw region after 5-mm activation of the bone-born expansion appliance.

the posterior area. The combined expander with miniscrews inserted lateral to the midpalatal suture, and conventional hyrax arms on the teeth showed the maximum transverse displacement. The rotational movement of the dentoalveolar unit was larger for the bone-borne devices with or without hyrax arms. SARPE without miniscrews demonstrated the most transverse displacement. The stresses around the appliances with miniscrews were more concentrated on the palate than on the alveolar ridge. They suggested

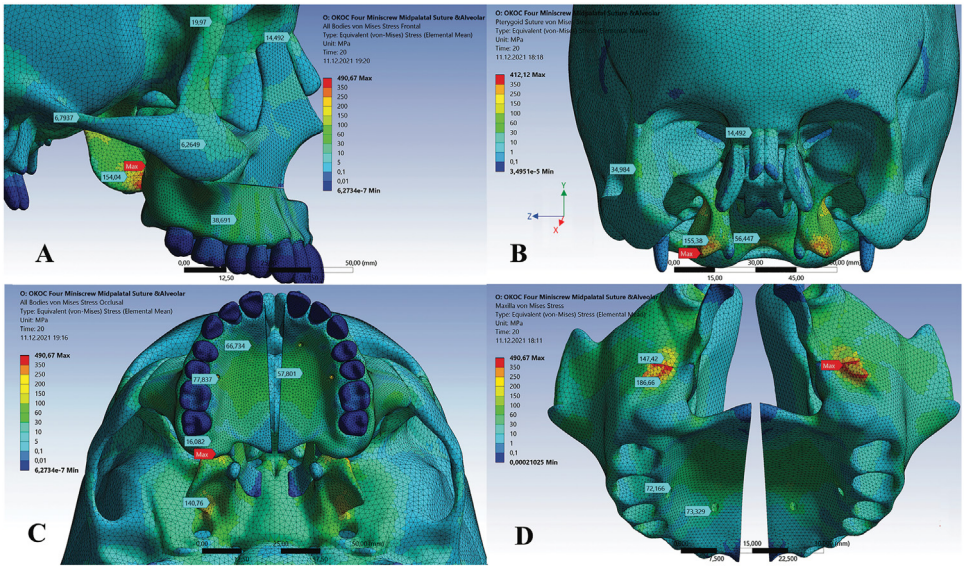


Fig 6. **A** and **C,** Model III: Unilateral stress distribution in the craniofacial structures and maxillofacial sutures; **B** and **D,** Unilateral stress distribution in the pterygomaxillary suture and screw region after 5-mm activation of the bone-born expansion appliance.

miniscrew-supported expanders for the effective treatment of maxillary transverse deficiencies.[29] Based on this result, miniscrew-supported expansion appliances were preferred in this study to compare the effects of SARPE.

In previous studies, an important impact of SARPE on the maxilla has been presented as the lateral rotational movement rather than the horizontal displacement.[8] This effect is attributed to applying force at the occlusal level, away from the center of rotation, of the traditional tooth-borne maxillary expansion appliances used in SARPE.[38] The maxilla showed a wedge-shaped opening with expansion in the current study, and the highest stress value was observed in the pterygomaxillary suture and miniscrew placement areas.

For more reliable results in FEA studies, a protocol similar to the clinical activation of the screw and nonlinear analysis is recommended.[29,38,43] Unlike a clinical application, only the first activation of the expansion screw (0.25-1.00 mm) was evaluated in most of the FEA studies that included SARPE simulations.[28,29,38] In these studies, stress distribution and amount of displacements in the craniofacial structure and the maxilla were investigated with the effect of the force (800-6000 gf) that occurs with only 1 activation of the screw.[40,43] In this study, 5 mm (20 activations of the screw) expansion was performed in a symmetrical model to reflect the clinical situation more accurately. Both principal and total von Mises stress values were compared with the previous studies.

When the literature was investigated, the stress and displacement results measured from craniofacial and maxillofacial sutures were relatively similar in FEA studies conducted for bone-borne expansion without PTMS in SARPE.[29,36,38] A study found 1.22 mm displacement for the transpalatal distractor appliance model and 0.87 mm for the alveolar crest supported appliance model because of a 1 mm opening of the expansion screw.[36] In this study, 1.38 mm displacement in model I and 1.97 mm displacement in model II was measured for the incisors at the same opening amount.

Möhlhenrich et al[36] found the highest stress was in the median and lateral pterygoid plates in the median and lateral osteotomy model. Our study measured the highest stress in the same regions except for the miniscrew area. Möhlhenrich et al[36] also stated that the stresses measured on the craniofacial structures were higher in the bone-supported expansion model, whereas the stress was lower in the alveolar crest model. They concluded that the force applied to the alveolar ridge reduces the stresses on the maxillofacial complex.[36] These results are consistent with this study.

Lee et al[29] observed the maximum stress values around the miniscrew area in the palatal suture (360 MPa) and around the miniscrew area in the alveolar ridge (46 MPa). In this study, 157 MPa was measured around the miniscrews in model I and 38 MPa in model II.

An FEA study[38] found 0.29 mm displacement for incisors with an alveolar ridge-located miniscrews-assisted palatal expander in SARPE with 0.5 mm expansion. This study measured a displacement of 0.98 mm for the incisors in model II, a similar model. This difference can be attributed to the modeling of the miniscrews and the direct application of the force through the appliance or different bone material properties, several mesh elements, and nodes.

Studies investigating the miniscrews placed on the alveolar ridge found reduced stresses around the screws and in the craniofacial structures.[29,38] These results are consistent with the findings in this study as well.

Some clinical implications can be drawn from this SARPE simulation; although a wedge-shaped expansion pattern was observed in all maxillary expanders, this form was found more prominent in the alveolar-located 2-miniscrew-assisted palatal expanders. Moreover, the maximum displacement was found at the incisors and anterior part of the maxilla for the same expander. This expander can be used for patients with severe constriction in the anterior region of the maxilla and/or crowding in the incisors.

The maximum displacement was found at the posterior region for the 4-miniscrew-assisted expander. This expander can be recommended, especially in patients with a severe posterior crossbite.

The minimum stress values were measured for the alveolar-located 2-miniscrew-assisted palatal expanders for all the craniofacial and maxillofacial structures. This result showed that 2-miniscrews-assisted expanders created less stress than the 4-miniscrew-assisted expanders, which is important in selecting the maxillary expansion appliance.

The accuracy of the solution in FEA largely depends on the number of elements in the model and the mesh convergence value. Gradually refining the mesh (dividing it into smaller elements) improves the results of the solution and converges the solution value toward a certain result, given enough iterations. Even if the element size is reduced in the convergence process, the solution value does not change after a stage. There are some situations in which the solution does not converge with mesh refinement. Singularity is one of these situations, and reducing the element size in the singularity error region to improve the mesh structure causes an increase in stress.

Singularity error refers to the location in which stress value is unbounded in a finite element model.[35] Boundary conditions (application of load to 1 point) or geometry and simplification of the model (nonuniform and/or sharp-edged surfaces) can be the causes of the singularity. In the bone model, there are nonuniform sharp-edged surfaces because of geometry. Because of the solver mathematical calculation errors in FEA, high-stress values are formed in areas with sharp corners.[35] The general model was divided into 1,461,017 elements; the maximum stress value was observed in a few elements (accumulated in the region of the pterygomaxillary suture) because the singularity error was not considered. In the analysis, these maximum stress values arising from the singularity error did not affect our results.

As a result of the bone's flexibility to load and self-healing property, maximum stress values do not accumulate at a single spot, as shown in the FEA results. Moreover, this FEA simulation did not include relapse after expansion, remodeling of the bones, effects of the soft tissues, muscles, and chewing forces. Therefore, results may differ from in vivo conditions. Displacements and stresses can be higher than clinical values. If these effects can be added to the boundary conditions in future FEA studies, the accuracy of the simulation will be increased. In vivo studies are needed to verify the results of this FEA study.

CONCLUSIONS

In conclusion, within the limitations of this FEA study;

1. An alveolar-located 2-miniscrew-assisted maxillary expander model showed the best stress distribution conditions for the craniofacial and maxillofacial structures.
2. The maximum stress value was measured in the midpalatal-located 2-miniscrew-assisted expander model for the ANS region.
3. The maximum stress value was measured in the 4-miniscrew-assisted expander for the median pterygoid plate region.
4. For the alveolar-located 2-miniscrew-assisted palatal expander model, the largest displacement was found at the incisors and anterior part of the maxilla.
5. For the 4-miniscrew-assisted expander model, the maximum displacement was found at the posterior region of the maxilla.

AUTHOR CREDIT STATEMENT

Osman Koç contributed to conceptualization, software, and original draft preparation; Hande Pamukçu contributed to conceptualization, original draft preparation, and supervision; and Azize Atakan Kocabalkan contributed to manuscript review and editing, methodology, and visualization.

SUPPLEMENTARY DATA

Supplementary data associated with this article can be found, in the online version, at https://doi.org/10.1016/j.ajodo.2022.12.001.

REFERENCES

1. Iodice G, Bocchino T, Casadei M, Baldi D, Robiony M. Evaluations of sagittal and vertical changes induced by surgically assisted rapid palatal expansion. J Craniofac Surg 2013;24:1210-4.
2. Ramieri GA, Nasi A, Dell'Acqua A, Verzé L. Facial soft tissue changes after transverse palatal distraction in adult patients. Int J Oral Maxillofac Surg 2008;37:810-8.
3. Altug Atac AT, Karasu HA, Aytac D. Surgically assisted rapid maxillary expansion compared with orthopedic rapid maxillary expansion. Angle Orthod 2006;76:353-9.
4. Kurt G, Altug-Ataç AT, Atac MS, Karasu HA. Changes in nasopharyngeal airway following orthopedic and surgically assisted rapid maxillary expansion. J Craniofac Surg 2010;21:312-7.
5. Byloff FK, Mossaz CF. Skeletal and dental changes following surgically assisted rapid palatal expansion. Eur J Orthod 2004;26:403-9.
6. Wertz RA. Skeletal and dental changes accompanying rapid midpalatal suture opening. Am J Orthod 1970;58:41-66.
7. Haas AJ. Palatal expansion: just the beginning of dentofacial orthopedics. Am J Orthod 1970;57:219-55.
8. Choi JY, Choo H, Oh SH, Park JH, Chung KR, Kim SH. Finite element analysis of C-expanders with different vertical vectors of anchor screws. Am J Orthod Dentofacial Orthop 2021;159:799-807.
9. Seong EH, Choi SH, Kim HJ, Yu HS, Park YC, Lee KJ. Evaluation of the effects of miniscrew incorporation in palatal expanders for young adults using finite element analysis. Korean J Orthod 2018;48:81-9.
10. Tausche E, Hansen L, Hietschold V, Lagravère MO, Harzer W. Three-dimensional evaluation of surgically assisted implant bone-borne rapid maxillary expansion: a pilot study. Am J Orthod Dentofacial Orthop 2007;131(4 Suppl):S92-9.
11. Lin L, Ahn HW, Kim SJ, Moon SC, Kim SH, Nelson G. Tooth-borne vs bone-borne rapid maxillary expanders in late adolescence. Angle Orthod 2015;85:253-62.
12. Zandi M, Miresmaeili A, Heidari A. Short-term skeletal and dental changes following bone-borne versus tooth-borne surgically assisted rapid maxillary expansion: a randomized clinical trial study. J Craniomaxillofac Surg 2014;42:1190-5.
13. Koudstaal MJ, Wolvius EB, Schulten AJM, Hop WCJ, Van der Wal KGH. Stability, tipping and relapse of bone-borne versus tooth-borne surgically assisted rapid maxillary expansion; a prospective randomized patient trial. Int J Oral Maxillofac Surg 2009;38:308-15.
14. Wilmes B, Nienkemper M, Drescher D. Application and effectiveness of a mini-implant- and tooth-borne rapid palatal expansion device: the hybrid hyrax. World J Orthod 2010;11:323-30.
15. Crismani AG, Bertl MH, Čelar AG, Bantleon HP, Burstone CJ. Miniscrews in orthodontic treatment: review and analysis of published clinical trials. Am J Orthod Dentofacial Orthop 2010;137:108-13.
16. Lim HJ, Choi YJ, Evans CA, Hwang HS. Predictors of initial stability of orthodontic miniscrew implants. Eur J Orthod 2011;33:528-32.
17. Wu TY, Kuang SH, Wu CH. Factors associated with the stability of mini-implants for orthodontic anchorage: a study of 414 samples in Taiwan. J Oral Maxillofac Surg 2009;67:1595-9.
18. Khosravanifard B, Rakhshan V, Raeesi E. Factors influencing attractiveness of soft tissue profile. Oral Surg Oral Med Oral Pathol Oral Radiol 2013;115:29-37.
19. Miyawaki S, Koyama I, Inoue M, Mishima K, Sugahara T, Takano-Yamamoto T. Factors associated with the stability of titanium screws placed in the posterior region for orthodontic anchorage. Am J Orthod Dentofacial Orthop 2003;124:373-8.
20. Wu Y, Xu Z, Tan L, Tan L, Zhao Z, Yang P, et al. Orthodontic mini-implant stability under continuous or intermittent loading: A histomorphometric and biomechanical analysis. Clin Implant Dent Relat Res 2015;17:163-72.
21. Holberg C, Winterhalder P, Rudzki-Janson I, Wichelhaus A. Finite element analysis of mono- and bicortical mini-implant stability. Eur J Orthod 2014;36:550-6.
22. Hong C, Lee H, Webster R, Kwak J, Wu BM, Moon W. Stability comparison between commercially available mini-implants and a novel design: part 1. Angle Orthod 2011;81:692-9.
23. Wilmes B, Ludwig B, Vasudavan S, Nienkemper M, Drescher D. The T-zone: median vs. paramedian insertion of palatal mini-implants. J Clin Orthod 2016;50:543-51.
24. Ludwig B, Glasl B, Bowman SJ, Wilmes B, Kinzinger GSM, Lisson JA. Anatomical guidelines for miniscrew insertion: palatal sites. J Clin Orthod 2011;45:433-41: quiz 467.
25. Becker K, Unland J, Wilmes B, Tarraf NE, Drescher D. Is there an ideal insertion angle and position for orthodontic mini-implants in the anterior palate? A CBCT study in humans. Am J Orthod Dentofacial Orthop 2019;156:345-54.
26. Wilmes B, Neuschulz J, Safar M, Braumann B, Drescher D. Protocols for combining the Beneslider with lingual appliances in Class II treatment. J Clin Orthod 2014;48:744-52.
27. Kyung HM, Park HS, Bae SM, Sung JH, Kim IB. Development of orthodontic micro-implants for intraoral anchorage. J Clin Orthod 2003;37:321-8: quiz 314.
28. Life science database archive: BodyParts3D. Available at: https://dbarchive.biosciencedbc.jp/jp/bodyparts3d/download.html. Accessed December 26, 2021.
29. Lee HK, Bayome M, Ahn CS, Kim SH, Kim KB, Mo SS, et al. Stress distribution and displacement by different bone-borne palatal expanders with micro-implants: a three-dimensional finite-element analysis. Eur J Orthod 2014;36:531-40.
30. Lee RJ, Moon W, Hong C. Effects of monocortical and bicortical mini-implant anchorage on bone-borne palatal expansion using finite element analysis. Am J Orthod Dentofacial Orthop 2017;151:887-97.
31. Holberg C, Steinhäuser S, Rudzki I. Surgically assisted rapid maxillary expansion: midfacial and cranial stress distribution. Am J Orthod Dentofacial Orthop 2007;132:776-82.
32. Hartono N, Soegiharto BM, Widayati R. The difference of stress distribution of maxillary expansion using rapid maxillary expander (RME) and maxillary skeletal expander (MSE)-a finite element analysis. Prog Orthod 2018;19:33.
33. Peterson J, Wang Q, Dechow PC. Material properties of the dentate maxilla. Anat Rec A Discov Mol Cell Evol Biol 2006;288:962-72.
34. Peterson J, Dechow PC. Material properties of the human cranial vault and zygoma. Anat Rec A Discov Mol Cell Evol Biol 2003;274:785-97.
35. Bi Z. Finite Element Analysis Applications: A Systematic and Practical Approach. 1st ed. Cambridge: Academic Press; 2018. p. 455-94.

36. Möhlhenrich SC, Modabber A, Kniha K, Peters F, Steiner T, Hölzle F, et al. Simulation of three surgical techniques combined with two different bone-borne forces for surgically assisted rapid palatal expansion of the maxillofacial complex: a finite element analysis. Int J Oral Maxillofac Surg 2017;46:1306-14.
37. Romanyk DL, Vafaeian B, Addison O, Adeeb S. The use of finite element analysis in dentistry and orthodontics: critical points for model development and interpreting results. Semin Orthod 2020;26:162-73.
38. Lee SC, Park JH, Bayome M, Kim KB, Araujo EA, Kook YA. Effect of bone-borne rapid maxillary expanders with and without surgical assistance on the craniofacial structures using finite element analysis. Am J Orthod Dentofacial Orthop 2014;145:638-48.
39. de Assis DS, Xavier TA, Noritomi PY, Gonçales ES. Finite element analysis of bone stress after SARPE. J Oral Maxillofac Surg 2014; 72:167.e1-7.
40. MacGinnis M, Chu H, Youssef G, Wu KW, Machado AW, Moon W. The effects of micro-implant assisted rapid palatal expansion (MARPE) on the nasomaxillary complex—a finite element method (FEM) analysis. Prog Orthod 2014;15: 52.
41. Muñoz GA. Lecture 7: Mesh quality and advanced topics.2015. Available at: https://www.academia.edu/16970000/mesh_quality_and_advenced_topics_ansys_workbench_16.0. Accessed January 3, 2020.
42. Erdemir A, Guess TM, Halloran J, Tadepalli SC, Morrison TM. Considerations for reporting finite element analysis studies in biomechanics. J Biomech 2012;45:625-33.
43. Han UA, Kim Y, Park JU. Three-dimensional finite element analysis of stress distribution and displacement of the maxilla following surgically assisted rapid maxillary expansion. J Craniomaxillofac Surg 2009;37:145-54.